

Finite Element Simulation of Real-time Health Monitoring of Steel Rod using Active Fiber Optic Sensors

Qixiang Tang¹, Cong Du², Xingwei Wang², and Tzuyang Yu¹

¹Department of Civil and Environmental Engineering

²Department of Electrical and Computer Engineering

University of Massachusetts Lowell

One University Ave, Lowell, MA, U.S.A 01854

ABSTRACT

Steel structure members are widely used in modern constructions. Crucial structure members (i.e., the steel frame or hoist in an oil platform) should be monitored frequently since deterioration of such members jeopardizes safety of human and leads to economic loss. An active fiber optic sensor (FOS) utilizing the photoacoustic effect has been proposed for actively generating surface ultrasonic waves. By combining this FOS with a FOS receiver, surface corrosion detection of steel structures using ultrasound can be accomplished. In this study, surface ultrasonic wave propagation behavior in intact and corroded steel rod was investigated using finite element method. Ultrasonic waves (radial displacements) were collected by different FOS receivers and compared with each other. Spacing of sensors were optimized based on the simulation results. A surface corrosion detection method for steel rod was developed.

INTRODUCTION

Steel structure members are widely used in modern infrastructures. Crucial structure members (i.e., the steel frame or hoist in an oil platform) should be monitored frequently since deterioration of such members jeopardizes safety of human and leads to economic loss. Traditional damage detection or monitoring methods, such as ultrasonic testing or eddy current, usually require bulky equipment. Moreover, engineers need to be sent to site in order to practice such methods.

An active fiber optic sensor (FOS) utilizing the photoacoustic effect has been proposed for actively generating surface ultrasonic waves [1] [2]. By taking the advantages of small size of FOS, Zou [3][4][5] proposed using this active FOS to detect surface corrosion of steel rebar. However, its application in steel rod requires an efficient sensing scheme. The aim of paper is to develop a corrosion detection scheme for steel rod structures using such active FOS. Finite element method (FEM) was applied for simulating surface ultrasonic waves propagation in steel rod models. Four receiver locations were distributed on the steel rod model. Radial displacement response was collected for detecting, locating surface corrosion. In this paper, FE modeling of intact and corroded steel rod models is first described. Design of FE models and the characterization of artificial corrosion are provided. A corrosion detection scheme is proposed based on the maximum net displacement response at locations of the fiber optic photoacoustic receiver. Finally, research findings are discussed.

FINITE ELEMENT SIMULATION

To study the wave propagation in intact and corroded rebars, FE models were designed and used. An intact steel model was created first with 705600 (linear hexahedral) C3D8 elements [6]. Fourteen corroded steel rod models were created by introducing artificial surface corrosion to the intact model. The two ends of all models were fixed and a sinusoidal pulse was applied at mid-span. Displacement responses at four locations were collected and analyzed. FE modeling details are described in the following.

Material Property and Geometry

The intact model was made of steel, property of which is provided in Table 1. The steel rod model was a 50 mm (1.97 in) cylinder with a diameter of 12.7 mm (0.5 in), as shown in Fig.1.

Table 1. Material's properties

	Steel	Rust
Density (kg/m ³)	7850	2610
Young's Modulus (MPa)	210,000	500
Poisson's ratio	0.3	0.3

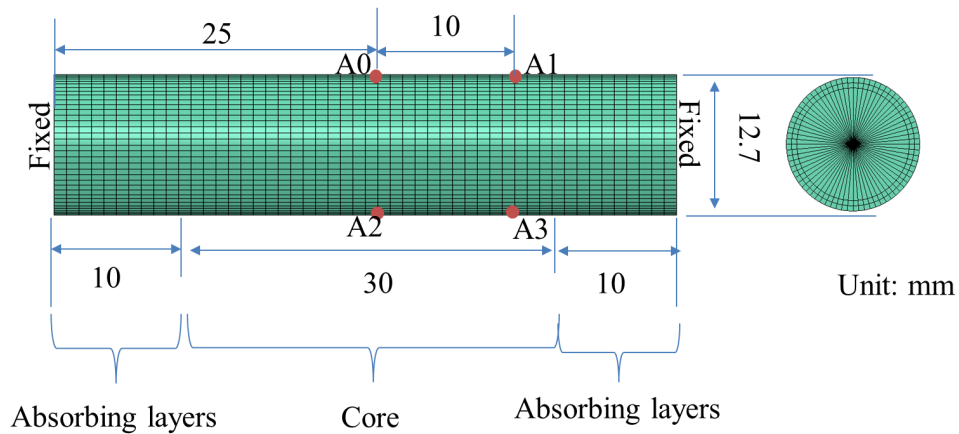


Fig. 1. Intact steel rod model

Artificial corrosion were introduced to the intact rod model in order to build corroded rod model. Material's properties were updated from steel to rust at corroded region. (The material of corrosion was defined as rust, as shown in Table.1.) To characterize a corroded region, four attributes were defined: location L^j , depth l_z , width l_θ , and thickness l_Q , as shown in Fig.2. L^1 was a corroded region on the top of the rod; it was 5 mm away from the mid-span. L^2 was located at mid-span. In the cylindrical coordinate system, the angle between L^1 and L^2 was 90° . Corrosion size was quantified by three parameters: depth $l_z = 2$ mm, width $l_\theta = 2.2$ mm, and thickness $l_Q = 2$ mm of the corroded region. The subscript indicates the axis on which the dimension describes. For example, l_z describes length of a corroded region on z-axis. (Note that the thickness l_Q of all corroded regions were fixed to 2mm.) Two corroded rod models with different corrosion location were listed in Table. 2.

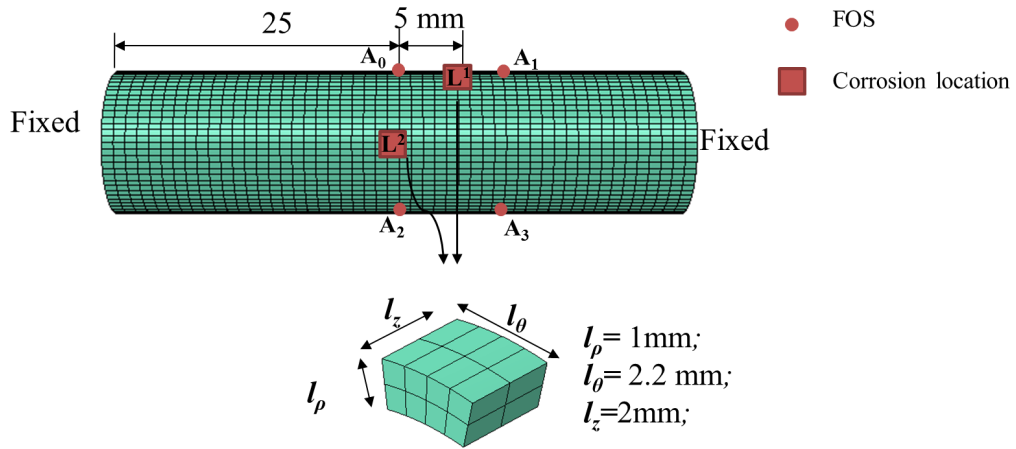


Fig. 2. Corroded steel rod model

Table 2. Considered corrosion models

Model CR	L^j	l_z (mm)	l_θ (mm)	l_ρ (mm)
1	L^1	2	2.2	2
2	L^2	2	2.2	2

Boundary Conditions and Loading

On each side of the rod, 10 mm (0.39 in) of absorbing regions were applied, as shown in Fig.3. These regions were created with absorbing layers using increasing damping (ALID)[3], and they serve as non-reflecting boundaries. When elastic waves propagated into an absorbing region, they were damped out. The material property in these regions is same as that of the core except additional damping. Each absorbing region contains 10 layers. The damping value of these layers linearly increases from the interface between the core and absorbing regions, to the fixed end.

Four receiver locations (A_i , where $i = 0, 1, 2$ or 3) were considered, as shown in Fig.1. In addition, a transducer was located at A_0 . A sinusoidal pulse (as shown in Fig.3) was applied at A_0 as input loading. Radial displacement in the time domain, at these four considered locations was collected.

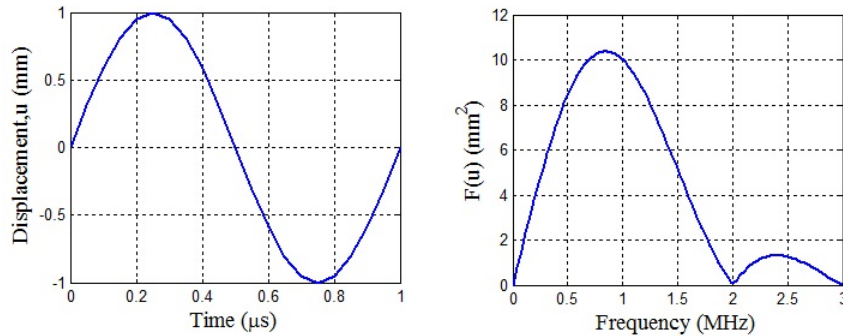


Fig. 3. Loading function in the time and the frequency domain

Net Displacement Response

Net displacement response δu_i^j was defined as the differential displacement between intact and corroded model at A_i (corrosion locates at L^j). It was calculated by Eq.(1).

$$\delta u_i^j = u_i^j - u_i^{int} \quad (1)$$

where u_i^j = displacement response of a corroded rod model at A_i , u_i^{int} = displacement response of intact model at A_i and δu_i^j = net displacement response of the corroded rod at A_i . To determine which pair is the best sensing scheme for detecting corrosion, a characteristic parameter named indicator (I_i^j) was proposed and defined as the normalized maximum net displacement response at A_i .

SIMULATION RESULTS

Net Displacement Response

Net displacement responses of each model were calculated using As an example, Figs.4 and 5 show net displacement responses at all four locations for model CR1 and CR2. In order to evaluate the effectiveness of locations A_i in terms of detecting corrosion, maximum net displacement responses from model CR1 and CR2 are summarized into Table 3. Note that the corroded region of model CR1 and CR2 has identical sizes.

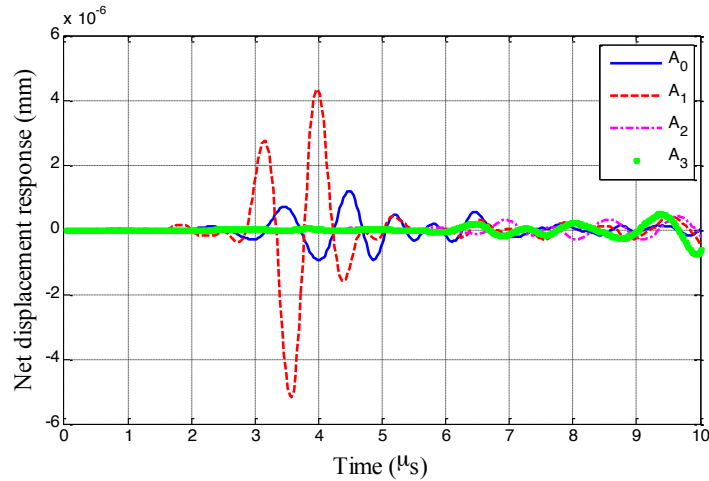


Fig. 4. Net displacement response of model CR1

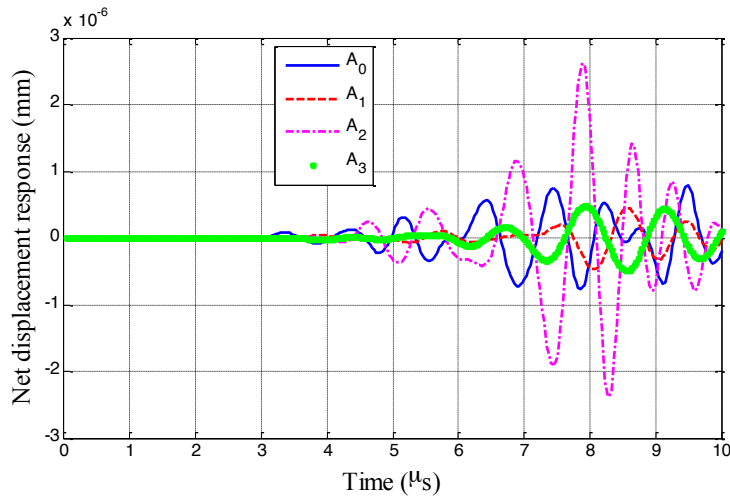


Fig. 5. Net displacement response of model CR2

Table 3. Maximum net displacement response $(\delta u_i^j)_{\max}$

Transducer	Receiver	Model CR1 ($\times 10^{-6}$ mm)	Model CR2 ($\times 10^{-6}$ mm)
A ₀	A ₀	0.64	2.09
A ₀	A ₁	3.05	1.33
A ₀	A ₂	0.59	3.09
A ₀	A ₃	0.94	0.97

Table 4. Indicator I_i^j of case 2 and CR9

Transducer	Receiver	Model CR1 (%)	Model CR2 (%)
A ₀	A ₀	0.8	4.93
A ₀	A ₁	36.45	15.92
A ₀	A ₂	3.15	16.14
A ₀	A ₃	8.74	9.01

Corrosion Detection

Evaluation of receiver locations for corrosion detection is achieved by comparing the maximum net displacement response and indicator I_i^j .

- Corrosion detection -- Indicator I_i^j at A₁ can be used to detect the presence of corrosion since it has high value of the indicator in model CR1 and CR2. From the definition, any non-zero value of I_i^j suggests the appearance of corrosion. However, the sensitivity of considered receivers changes for same levels of corrosion. In Table 4, A₁ always has great values in both model CR1 and CR2.
- Corrosion location -- For considered corrosion locations (L^j), the greatest net displacement response $(\delta u_i^j)_{\max}$ at A₁ predicted corrosion located at L^1 ; the greatest $(\delta u_i^j)_{\max}$ at A₀ or A₂ predicts corrosion location at L^2 . It was found that when the corrosion is between a receiver and the transducer, $(\delta u_i^j)_{\max}$ of this receiver have the greatest value against the values of other receivers. For example, in model CR2 and with a $(\delta u_i^j)_{\max}$ value at A₁, corrosion was predicted to be located between A₁ (receiver) and A₀ (transducer). From Table 4, value of A₁ is much greater than any other locations. Similarly, in model CR2, corrosion locates between A₂ (receiver) and A₀ (transducer). (A₀ is also a receiver in this case.) In Table 3, $(\delta u_i^j)_{\max}$ of both A₀ and A₂ are greater than other receivers.
- In the frequency domain (see Figs.6 and 7), it was found that frequency response was affected more when corrosion locates between the transducer and receiver. Corrosion locates between transducer and receiver has less effect on frequency response. As an example, Fig.7 shows the frequency response at A₂. Frequency response of model CR1 was almost overlapped with the one of intact model. However, frequency response of model CR2 (when corrosion is between the transducer and receiver) had large different from the one of intact model.

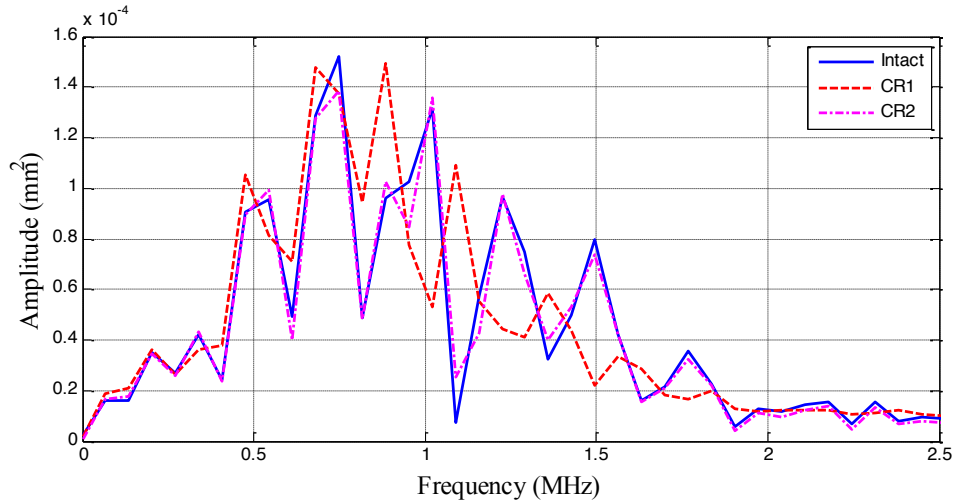


Fig. 6. Frequency responses at A_1

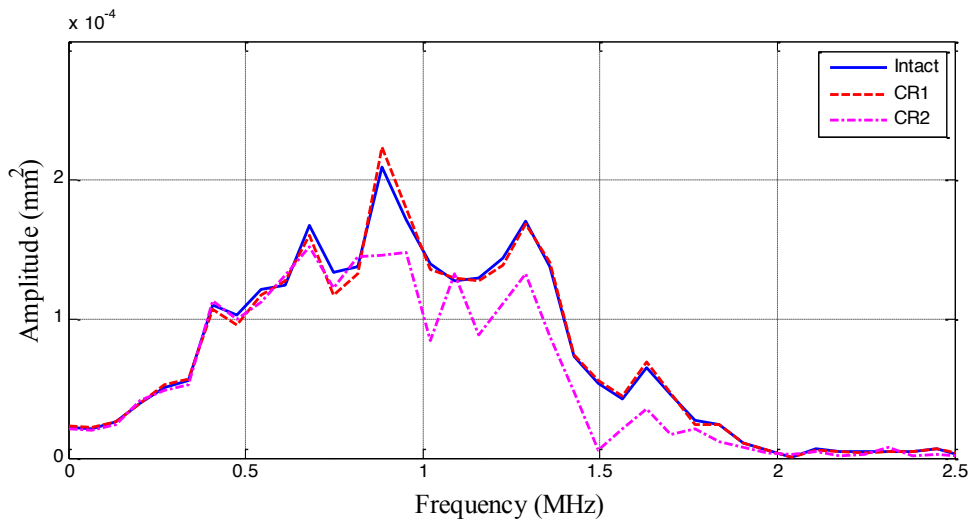


Fig. 7. Frequency responses at A_2

- By applying Gaussian curve fitting to the frequency response of each model, center frequencies were found [6], as shown in Table 5. It was found that, center frequency response was reduced when corrosion located between the transducer and receiver. For example, when corrosion located between A_0 and A_1 , center frequency reduced from 1.01MHz to 0.78 MHz.

Table 5. Center frequencies of each model

Model CR	Intact Rod (MHz)	Model CR1 (MHz)	Model CR2 (MHz)
A_0	0.88	0.87	0.89
A_1	1.01	0.78	0.79
A_2	0.87	0.94	0.65
A_3	1.1	0.83	1.09

Summary

From the FE simulations, both time domain and frequency domain analysis suggest that a pair of transducer and the receiver provide higher corrosion detection efficiency when the corrosion locates between them. The best sensing scheme was determined to be 'transducer - corrosion - receiver'. Therefore, it's good to put receivers at both A_1 and A_2 , such that corrosions between A_0 and A_1 , or A_0 and A_2 can be detected. At any receiver (A_1 or A_2), none-zero value of net displacement response ($\delta u_i^j \neq 0$) indicates the existence of corrosion between the transducer A_0 and this receiver.

In this paper, detection scheme utilizing the maximum net displacement response (δu_i^j) were evaluate in both time domain and frequency domain. This detection scheme can be used as guidance for detecting surface rust of steel rod structure using small sensors such as FOS.

ACKNOWLEDGEMENT

The authors would like to thank the National Science Foundation (NSF), Division of Civil, Mechanical and Manufacturing Innovation (CMMI) for partially supporting this research through Grant CMMI-1401369.

REFERENCES

1. Mendez, A., and T. Graver, "Overview of fiber optic sensors for NDT applications," *Proceedings of IV NDT Panamerican Conference*, Buenos Aires, Argentina, October 2007.
2. Zou, X., A. Chao, Y. Tian, N. Wu, H. Zhang, T. Yu, X. Wang, "An experimental study on the concrete hydration process using Fabry-Perot fiber optic temperature sensors," *Measurement*, Volume 45, Issue 5, June 2012.
3. Zou, X., A. Chao, N. Wu, Y. Tian, T. Yu and X. Wang, "A novel Fabry-Perot fiber optic temperature sensor for early age hydration heat study in Portland cement concrete," *Smart Structures and System*, Volume 12, Issue 1, July, 2013.
4. Zou, X., N. Wu, Y. Tian, X. Wang, "Broadband miniature fiber optic ultrasound generator," *Optical Express*, Volume 22, pp. 18119-18127, 2014.
5. Zou, X., T. Schmitt, D. Perloff, N. Wu, T. Yu, and X. Wang, "Nondestructive corrosion detection using fiber optic photoacoustic ultrasound generator," *Measurement*, Volume 62, pp.74-80, 2015.
6. ABAQUS v6.11 Analysis User's Manual, "ABAQUS Documentation," Dassault Systèmes, Providence, RI, USA.
7. Tang. Q and T. Yu. "Finite element simulation of ultrasonic waves in corroded reinforced concrete for early-stage corrosion detection", *Proc. SPIE 10169, Nondestructive Characterization and Monitoring of Advanced Materials, Aerospace, and Civil Infrastructure 2017*, 101691N, April 2017;